Analyst

Accepted Manuscript

ROYAL SOCIETY OF CHEMISTRY

www.rsc.org/analyst

Journal Name

ARTICLE

Rapid Microstructure Characterization of Polymer Thin Films with 2D-Array Multifocus Raman Microspectroscopy

Ashok Zachariah Samuel,[a, c] Sohshi Yabumoto,[b, c] Kenichi Kawamura,[b] and Koichi Iwata[*a]

Raman imaging is one of the very informative methods for the characterization of chemically and structurally heterogeneous materials without employing specific molecular labels. Multifocus Raman imaging is one of the fast-imaging alternatives to the conventional single point mapping technique. Since multiple focal points probe the sample simultaneously, this imaging methodology is faster compared to single point mapping. We further demonstrate the efficiency of this methodology by investigating the morphological features of porous PMMA film. A Raman image of 50X50 μm^2 area was obtained in less than 4 minutes (with 10X10 multifocus configuration). Importantly, a 100X100 μm^2 area could now be analyzed in minutes while a similar Raman image in single point mapping would take hours to days. Optical sectioning using multifocus Raman imaging reveals unique hierarchical features of the porous polymer thin film. Larger pores are limited to the surface and the inner bulk exhibits characteristic small-pores and interconnected highly porous morphology. The fast multifocal Raman imaging would be advantageous to the diverse field of scientific disciplines where the speed of image acquisition remains a challenge despite the unparalleled specificity and sensitivity of Raman spectroscopy.

Introduction

Chemical imaging has become one of the most desirable characterization tools in material science and biophotonics since it allows simultaneous investigations of morphology and spatial distribution of functional entities (chemical species) based on molecular fingerprinting. Among diverse spectral imaging techniques developed, Raman imaging is benefited by rich information on molecular structure, negligible interference from water signals and noninvasiveness. Unprecedented sensitivity and higher specificity of Raman spectroscopy for monitoring bioactivity of living cells,[1] cancer diagnosis,[2] carbon based material[3] characterization etc. have already been demonstrated. Spectral imaging based histopathology[4] and on-table tumor imaging during surgery[5] are becoming increasingly popular in medical fields. Despite the obvious potential of Raman spectroscopy, the technique has witnessed a setback due to speed of image acquisition.

There were several attempts to increase the speed of image acquisition by adopting line- or slit-scanning or global illumination.[6] In the line scanning methodology, sample is illuminated using a line focus and the spatial region along the illuminated line is resolved by CCD pixels. In the wide field illumination methodology, a laser illuminates the entire field of view and Raman image is directly acquired using an imaging CCD. Here the spectral region (spectral resolution <10 cm^{-1}) of interest is selected using a band filter (e.g. acousto-optic tunable filter (AOTF) and liquid crystal tunable filter (LCTF)). The wide field illumination acquires Raman images rapidly but it does not provide Raman spectrum simultaneously and for obtaining the spectrum one has to resort to point scanning. Very recently Okuno and Hamaguchi have demonstrated multifocus methodology with a microlens array in Raman microscopy as a fast Raman imaging alternative to conventional single point mapping.[7] The multifocus excitation methodology is also utilized in the field of second-harmonic generation microscopy,[8] fluorescence microscopy,[9] coherent anti-Stokes

Raman scattering (CARS) microscopy,[10] and two-photon microscopy.[11] Rapid confocal Raman imaging by a multi-foci scanning method with a pair of galvo mirrors has also been developed.[12] In the multifocus Raman imaging methodology, the spatial region of interest is illuminated by multiple laser lines; each of which is separately focused at a different spatial spot. Raman scattering from these illuminated spots are collected using a fiber optic array. This technique has the advantage of obtaining full Raman spectrum simultaneously with the Raman images.

In this study we have constructed a 2D-array multifocus Raman microscope that consists of 441 individual focal points at the focal plane. A single laser beam is split into 21X21 multiple beams with a diffractive optical element (DOE).[13] Each of these individual beams is then focused using a microscope objective into different regions (multiple foci) of the sample forming a 2D array of laser spots (21X21). Our study revealed unique hierarchical features of the porous PMMA film prepared *via.* water phase separation strategy.

Experimental section

Optical Set up

The optical set up of the current microscope is briefly described in Figure 1. Output from a continuous wave diode-pumped solid-state (DPSS) laser (532 nm, 5 W) was split into 21X21 multiple laser line-array, using a diffractive optical element (DOE)[13] formed in a square SiO_2 plate, 11 mm in diameter and 3 mm in thickness. The 2D laser line array was then fed into a microscope objective (40X) and focused onto the sample. The image of the array of foci is shown as the inset of Figure 1. The Raman scattering from each of these spots was collected using a fiber bundle (21X21; 50 μm in diameter) and was recorded using a dispersive spectrometer (transmission-grating of 1300 lines/mm) and a CCD detector (TE cooled down to -100 degrees in Celsius, 2048 x 2048 array, 13.5 X 13.5 $μm^2$ pixel area, back-illuminated; Andor). The 2D array of the fiber bundle was rearranged to a 1D array along the entrance slit direction in order to couple it to the spectrometer. A typical laser power of 1.5-2 W (at the laser) was used in the present study for imaging (~3 mW per laser spot). Each illuminated focal spot probes a specific sample volume and reveals space resolved (diffraction limited) molecular information.

Preparation of the porous PMMA film

Porous polymer film was prepared in the following way using the methodology reported earlier.[14] 10 mL of PMMA solution (3wt% in THF) was poured into a clean Petri dish followed by addition of 270 μL of the sodium dodecyl sulphate (SDS) solution (8.5 mM). The solution was then swirled to ensure homogenization. The Petri dish containing the solution was covered with a beaker (500 ml) saturated with THF vapor to effect slow solvent evaporation. The film preparation was carried out at the room temperature. THF and water are completely miscible but they differ in their volatility. This causes THF to evaporate faster compared to water during the early stage of film formation. As THF composition reduces in the solution, due to evaporation, phase separation of water and the polymer solution occurs. These water droplets (stabilized by the surfactant molecules) are believed to act as templates to create the pores. Eventual evaporation of water results in the

formation of porous features in the film. Surfactant molecules organize at the interface between water and polymer providing functionality at the inner surface of pores.[14]
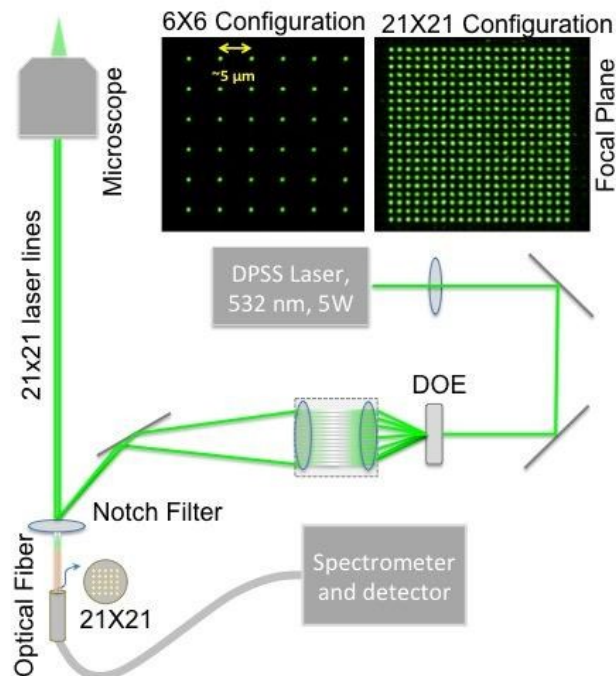

Figure 1. The basic optical set up of the multifocus Raman microscope constructed. Images of the multiple focal points formed at the sample plane for both the 21X21 and 6X6 configurations are provided as the inset.

Results and Discussion

The multifocus configuration consists of 21X21 focal point array (441 foci) with approximately 1 μm spacing between the focal points. Raman images of the porous PMMA film were recorded with this configuration. The microstructural features were not evident in the images, indicating a possible cross talk between foci. The scattered light from one illuminated focal region was also captured by optical fibers designed to collect information from neighboring focal points.

Possibility of the cross talk was examined by performing a single point illumination (SPI) experiment. The strategy employed in the single point illumination (SPI) experiment is pictorially illustrated in Figure 2. Green lines in the figure represents the multiple (21X21) laser beams generated using a DOE. The red circles (in the yellow rectangle) represent the 21X21 focal points corresponding to these individual laser beams if they were focused on to the sample. However, out of the 21X21 lines only a single laser beam was selected for the single point illumination (SPI) experiment. Placing a mask in front of DOE allowed separation of the single laser beam. A green dot in the yellow rectangle (depicting a sample in the figure) indicates the sample region illuminated by this laser beam. The Raman scattering from this single focus was collected using the whole 21X21 fiber bundle. In the current optical set up (Figure 1), each fiber is designed to collect the scattering from a specific focal point at the sample. Therefore, in the SPI experiment, if the spatial specificity is maintained,

Raman scattering should only be captured by a single optical fiber corresponding to the focal point illuminated. Then, the corresponding SPI Raman image should have only one bright pixel.
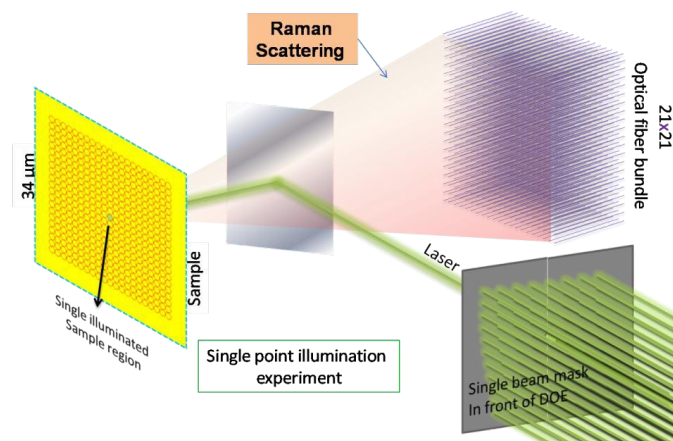

Figure 2. Schematic representation of single point illumination (SPI) experiment. The sample was illuminated using a single laser beam (green line), although the collection was performed using the 21X21 optical fiber bundle.

The SPI experiments were conducted on silicon wafer and PMMA porous films. Only one bright pixel was observed in the SPI Raman image of the Si wafer confirming the spatial specificity (Figure S1). However, when the same experiment was conducted on a porous PMMA film, considerable cross-talk was observed (Figure 3A; also *see* Figure S2). The cross-talk reduced considerably (< 5%) at a distance of ~5 micron from the illuminated spot (Figure 3A). On hard and opaque Si wafer surface the diffuse scattering and other undesired scattering effects might not be pronounced. But on a softer semitransparent surface like PMMA-film diffuse scattering effect will be prominent. The diffuse scattering phenomenon is effectively utilized in spatially offset Raman spectroscopy (SORS) technique to obtain subsurface information by providing an offset between excitation and collection points.[15] Such diffusively scattering photons introduce cross-talk in the present multifocal configuration. Hence the 21X21 configuration was changed to a 6X6 configuration using a mask in front of the DOE (see supporting information S3; Figure S3). This configuration provides approximately a 5 micron gap between focal points. In order to probe the region between two focal points, we used the interpolation technique (Figure S4), where we raster scan the sample region with the 2D multifocal array. The number of sampling points between two foci is denoted as interpolation number (or simply interpolation) (Figure S4). The Raman images of a patterned silicon wafer and polystyrene beads recorded with the modified multifocal (6X6) configuration applying 10X10 interpolation are provided in Figures 3B and 3C along with the corresponding white light images (3D and 3E). It is clear by comparing the Raman images with the corresponding white light images that the spatial specificity is maintained during the imaging with the current Raman microscope. The dimensions estimated from the images match well with the expected dimensions of the substrate (Si wafer 3 µm and PS beads 3 µm (FWHM)). However, fluctuation in the location of PS beads seems to have affected

its Raman image; the size of PS beads appears slightly larger in the Raman image.

We have then employed the 6X6 multifocus Raman microscopy to examine the morphological features of porous polymethylmethacrylate (PMMA) films. The porous features are clearly visible in the Raman image obtained with the 6X6 configuration (Figure 3F). It should be noted that the image with the 21X21 multifocal configuration did not reveal any microstructural features (Figure 3H; The Raman image of the porous film represents the intensity of the 810 cm^{-1} PMMA peak). While, A comparison between the white light image of the porous film and the corresponding Raman image is provided in the supporting information S6. The 6X6 multifocal configuration measures 33.8X33.8 µm^2 sample region. This Raman image was recorded with 20 seconds per acquisition (per frame) and the complete imaging was obtained in approximately 15 minutes (~33X33 µm^2) with the diffraction limited resolution. When the exposure time was reduced from 20 sec to 1 sec per acquisition the total scanning time was reduced to approximately 4 minutes (for ~33X33 µm^2 area with the 6X6 configuration; for 50X50 µm^2 area with the 10X10 configuration).
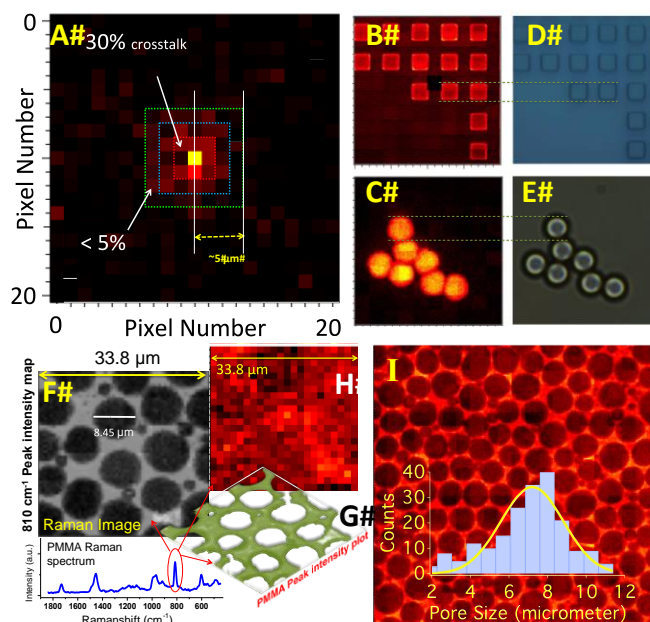

Figure 3. Spectral cross-talk observed in a porous PMMA film (A, SPI experiment). Raman images of patterned silicon wafer (B) and polystyrene beads (C) with the corresponding white light images (D and E, respectively). Raman image of porous polymer film recorded with the 6X6 multifocal configuration (F). The Raman spectrum of PMMA is given below the image. A representative cartoon for the porous film (G). Raman image of porous PMMA film recorded with the 21X21 configuration (H). The full dimension of the figures A, B, C, D, E, F and H is common with 33.8 µm. Porous morphology is not evident in the Raman image due to the cross-talk. A large area Raman image of porous polymer film (I, 100X100 µm^2). The estimated pore size distribution is shown as the inset. The plots A, F, H, I represent the intensity of the 810 cm^{-1} PMMA Raman band. The plots B and C represent the intensity of the 520 cm^{-1} Raman band of silicon and the 1001 cm^{-1} Raman band of polystyrene, respectively.

A large area scan (~100X100 μm²) requires tiling and interpolation simultaneously (see supporting information S5). A Raman image of porous film recorded using a 6X6 configuration, 3X3 tiling and 10X10 interpolation is provided in Figure 3I. We have estimated the pore size distribution from the image and the average pore size has been found to be 7.0 μm with a broad distribution (Figure 3I inset). The estimated pore size is within the range expected for films prepared under similar conditions.[14] Importantly, this Raman image (6X6 configuration, 10X10 interpolation, 100X100 μm² area) was acquired in approximately 97 minutes with a 5 sec exposure time per frame (32,400 spectra). The speed of imaging cannot be directly compared between the single focus and multifocus methodologies. The speed of imaging depends on several factors such as number of pixels per image, excitation power per focus, exposure time, and scattering cross-section of the sample, as well as the time required for stage movements and data readout. However, under similar conditions, a multifocus configuration with *n*-focal points is, in principle, *n* times faster than conventional the single point mapping. Thus a 6X6 2D array multifocal configuration is 36 times faster and a 10X10 configuration is 100 times faster than the single focus mapping. The Raman spectra recorded with different exposure times and an image recorded with a 200 ms exposure time per acquisition is given in Figure 4.
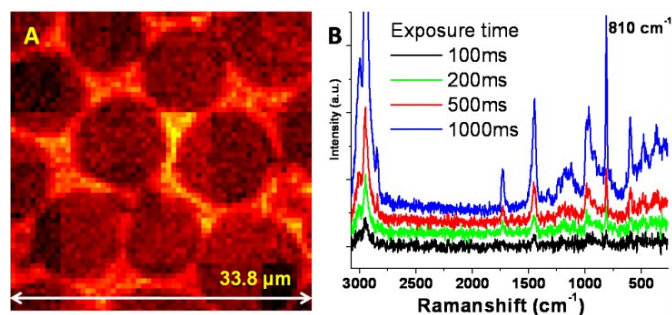

Figure 4. A) Raman image of the porous polymer film obtained with 200 ms exposure time per frame. The plot represents intensity of the 810 cm^{-1} PMMA peak. B) Raman spectra of PMMA film at different exposure times.
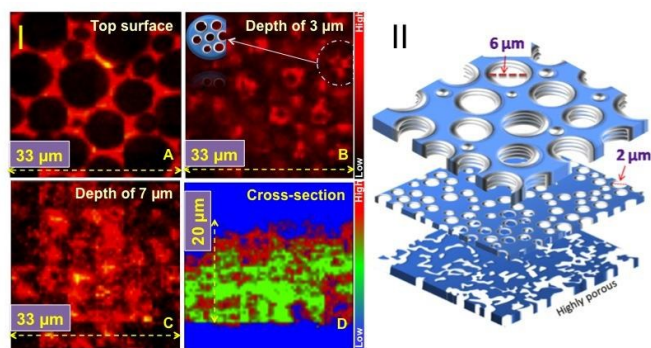

Figure 5. I) Raman images of porous polymer film at different depths (A, B and C) and a model depiction of the smaller pores (B inset). Raman image of a cross-section of the porous thin film (D). All the plots represent intensity of the 810 cm^{-1} PMMA peak. II) A cartoon depiction of a possible hierarchical porous morphology of PMMA films. (For image processing details see supporting information S5; Figure S9)

The 3D shape of the pores and inner bulk structure of the thin films were analyzed by optical sectioning using the multifocus Raman microscope. We have recorded the Raman images of the thin film by moving the focal plane stepwise (1 micron step) in the z-direction into the film. Although it is difficult to incorporate a confocal pinhole array in the current optical set-up, the optical fiber with a diameter of 50 μm functioned, at least partially, as a practical pinhole, which allowed the depth profiling. The Raman images obtained at different depths are provided in Figure 5I. The large pores are present only at the surface and they disappear at a depth of 2-3 microns (see also supporting information S4). As we go deeper into the film the depth resolution apparently becomes poorer, which is in agreement with the refraction induced variations in the focal volume (Figure S7).[16] However, the depth profiling of the top surface indicates that the shape of these pores is distinctly different (cylindrical; see Figure S8) when compared to the "cup shaped" porous structures typically observed in porous polymer films.[17] This observation agrees with the fluorescence microscopic images reported previously.[14] The inner bulk structure of the porous thin film is found to be distinctly different from the top layer. Interconnected smaller-pores are observed at a depth of 3 microns (Figure 5I) from the surface. Morphology changed to narrow channel type interconnected futures in the deeper regions of the film. The highly porous nature of the film is also evident from the Raman image of the film cross-section (Figure 5ID). A model explaining the observed features is provided in the Figure 5II. These observed hierarchical[18] mesoporous features are unique and are useful in variety of applications including gas storage, separation etc.[19]

Conclusions

In conclusion we have demonstrated a novel multifocus Raman imaging methodology for fast Raman image acquisition, which is 36 (6X6 configuration) to 441 (21X21 configuration) times faster than the single point mapping. A cross-talk problem was identified and was solved by providing adequate spacing between focal points. We have further employed this technique to explore morphological characteristics of porous PMMA thin film prepared via water phase separation strategy. Unique hierarchical porous morphology is revealed in our study. Moreover, the multifocus Raman imaging demonstrated here would be a useful tool for researchers in diverse fields of scientific disciplines.

Acknowledgements

Notes and references

ᵃ Department of Chemistry, Faculty of Science, Gakushuin University, 1-5-1 Mejiro, Toshima-ku, Tokyo 171-8588, Japan..

ᵇ Tokyo Instruments, Inc., 6-18-14 Nishi-Kasai, Edogawa-ku, Tokyo 134-0088, Japan.

c Present address, Department of Applied Chemistry and Institute of Molecular Science, National Chiao Tung University, 1001 Ta-Hsueh Road, Hsinchu 30010, Taiwan.

Analyst Accepted Manuscript

Electronic Supplementary Information (ESI) available: Results of the single point illumination experiment, additional information on the interpolation and tiling, etc. is provided in the supporting information.

1. (a) Y. Huang, T. Karashima, M. Yamamoto and H. Hamaguchi, *Biochemistry* 2005, **44**, 10009; (b) Y. Naito, A. Toh-e and H. Hamaguchi, *J. Raman Spectrosc.* 2005, **36**, 837.

2. a) Y. K. Min, T. Yamamoto, E. Kohda, T. Ito and H. Hamaguchi, *J. Raman Spectrosc.* 2005, **36**, 73; (b) A. S. Haka, K. E. Shafer-Peltier, M. Fitmaurice, J. Crowe, R. R. Dasari and M. S. Feld, *Proc. Natl. Acad. Sci. USA* 2005, **102**, 12371; (c) L. M. Almond, J. Hutchings, N. Shepherd, H. Barr, N. Stone and C. Kendall, *J. Biophotonics* 2011, **4**, 685.

3. M.S. Dresselhaus, A. Jorio and R. Saito, *Annu. Rev. Condens. Matter Phys.* 2010, **1**, 89.

4. J. Hutchings, C. Kendall, N. Shepherd, H. Barr and N. Stone, *J Biomed. Opt.* 2010, **15**, 066015.

5. K. Kong, C. J. Rowlands, S. Varma, W. Perkins, I. H. Leachc, A. A. Koloydenko, H. C. Williams and I. Notingher, *Proc. Natl. Acad. Sci. USA* 2013, **110**, 15189.

6. (a) M. Bowden, D. J. Gardiner, G. Rice and D. L. Gerrard, *J. Raman Spectrosc.* 1990, **21**, 37; (b) D. K. Veirs, J. W. Ager III, E. T. Loucks and G. M. Rosenblatt, *Appl. Opt.* 1990, **29**, 4969; (c) D. N. Batchelder, C. Cheng and G. D. Pitt, *Adv. Mater.* 1991, **3**, 566; (d) P. J. Treado, I. W. Levin and E. N. Lewis, *Appl. Spectrosc.* 1992, **46**, 1211; (e) G. J. Puppels, M. Grond and J. Greve, *Appl. Spectrosc.* 1993, **47**, 1256; (f) M. D. Schaeberle, H. R. Morris, J. F. Turner and P. J. Treado, *Anal. Chem.* 1999, **71**, 175A; (g) S. Schlucker, M. D. Schaeberle, S. W. Huffman, I. W. Levin, *Anal. Chem.* 2003, **75**, 4312; (h) K. Hamada, K. Fujita, N. I. Smith, M. Kobayashi, Y. Inouye, S. Kawata, *J. Biomed. Opt.* 2008, **13**, 044027; (i) G. Falgayrac, B. Cortet, O. Devos, J. Barbillat, V. Pansini, A. Cotten, G. Pasquier, H. Migaud and G. Penel, *Anal. Chem.* 2012, **84**, 9116.

7. M. Okuno and H. Hamaguchi, *Optics Letters* 2010, **35**, 4096.

8. M. Kobayashi, K. Fujita, T. Kaneko, T. Takamatsu, O. Nakamura and S. Kawata, *Opt. Lett.* 2002, **27**, 1324.

9. T. Tanaami, S. Otsuki, N. Tomosada, Y. Kosugi, M. Shimizu and H. Ishida, *Appl. Opt.* 2002, **41**, 4704.

10. T. Minamikawa, M. Hashimoto, K. Fujita, S. Kawata and T. Araki, *Opt. Express* 2009, **17**, 9526.

11. B. Broek, B. Ashcroft, T. H. Oosterkamp and J. Noort, *Nano Lett.* 2013, **13**, 980.

12. (a) J. W. Kang, N. Lue, C. R. Kong, I. Barman, N. C. Dingari, S. J. Goldfless, J. C. Niles, R. R. Dasari, M. S. Feld, *Biomed. Opt. Exp.* 2011, **2**, 2484; (b) L. Kong, P. Zhang, J. Yu, P. Setlow and Y. Q. Li, *Appl. Phys. Lett.* 2011, **98**, 213703. (c) L. Kong, P. Zhang, P. Setlow, Y. Li, *J. Biomed. Opt.* 2011, 16, 120503.

13. L. Sacconi, E. Froner, R. Antolini, M. R. Taghizadeh, A. Choudhury and F. S. Pavone, *Optics Letters* 2003, **28**, 1918.

14. A. Z. Samuel, S. Umapathy and S. Ramakrishnan, *ACS Appl. Mater. Interfaces* 2011, **3**, 3293.

15. P. Matousek, M. D. Morris, N. Everall, I. P. Clark, M. Towrie, E. Draper, A. Goodship and A. W. Parker, *Appl. Spectrosc.* 2005, **59**, 1485.

16. N. J. Everall, *Appl. Spectrosc.* 2000, **54**, 1515.

17. M. S. Park, W. Joo and J. K. Kim, *Langmuir* 2006, **22**, 4594.

18. H. Sai, K. W. Tan, K. Hur, E. Asenath-Smith, R. Hovden, Y. Jiang, M. Riccio, D. A. Muller, V. Elser, L. A. Estroff, S. M. Gruner and U. Wiesner, *Science* 2013, **341**, 530.

19. D. Wu, F. Xu, B. Sun, R. Fu, H. He and K. Matyjaszewski, *Chem. Rev.* 2012, **112**, 3959.

Graphical abstract artwork for Analyst

Ashok, Yabumoto, Kawamura, and Iwata